

# Photonic Mixers for Wide Bandwidth RF Receiver Applications

Anthony C. Lindsay, *Member, IEEE*, Geoff A. Knight, *Member, IEEE*,  
and Stephen T. Winnall, *Student Member, IEEE*

**Abstract**—Optoelectronic mixers can exhibit a very wide bandwidth of operation with significantly reduced third-order intermodulation products. A 20-GHz bandwidth optoelectronic mixer has been constructed and characterized. The third order intermodulation terms were demonstrated to be more than 70 dB below the I.F. output. The mixer was then incorporated into a simple superheterodyne receiver architecture, which was shown to have a tangential sensitivity of  $\sim 66$  dBm and a compressive dynamic range of 44 dB. System limitations and possible improvements are discussed.

## I. INTRODUCTION

OPTOELECTRONIC TECHNOLOGIES are rapidly maturing to the stage where fiber optic links with very wide bandwidth, good RF sensitivity and reasonable dynamic range are attainable. While utilizing fiber links simply as wideband information “pipelines” is of itself useful, the next stage in the evolution of this technology for RF receiver applications lies in using optical techniques to undertake some form of signal processing in order that the output from the fiber represents processed information, rather than simply a reproduction of the electromagnetic environment.

Fundamental requirements in many defence receiver systems are for very wide bandwidth, wide dynamic range and high sensitivity. These conflicting demands mean that several different technologies are often needed to adequately cover the spectral regime of interest, which is traditionally 1–18 GHz for disciplines such as microwave electronic warfare (EW). Only two technologies—monolithic microwave integrated circuits (MMIC) and photonics—have the intrinsic capability to cover this bandwidth (and more) in individual devices. Hybrid systems which exploit the beneficial aspects of both technologies will probably be the optimal route to realizing new receiver architectures that meet future needs.

The well-defined sinusoidal transfer function of integrated optical modulators means that these devices can be used to produce RF mixers that exhibit reduced third-order intermodulation products between the local oscillator (LO) and RF signals, as was initially demonstrated in [1]. A stated advantage of using such a mixer in a wide bandwidth superheterodyne receiver architecture is the possibility of enhanced dynamic range, which arises as a consequence of the reduced

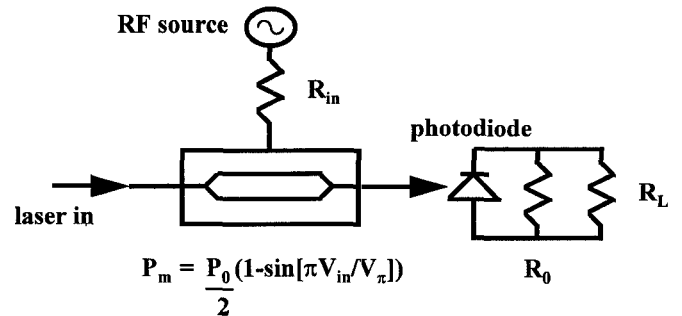


Fig. 1. Simple model for an externally modulated fiber optic link.

harmonic and intermodulation content from the strong LO-RF mixing process.

It is important that the potential for usefully implementing novel photonic technologies be analyzed not only at the component level but also at the full system level, in order to determine whether the promise demonstrated by individual components such as photonic mixers is actually realizable.

In this paper the construction and characterization of a 20-GHz optoelectronic mixer is reported and its incorporation into a simple superheterodyne receiver architecture is demonstrated. The system performance is analysed and a number of systems considerations are addressed.

## II. THEORY

### A. Wideband Fiber Optic Link

The model used for the wideband fiber optic link is shown in Fig. 1. A simple expression for the RF link gain  $\rho_G$  is derived in the Appendix as

$$\rho_G = R_{in} R_L \left( \frac{\pi r P_0 \alpha_{m1} \alpha_{opt}}{2 V_\pi} \right)^2 \left( \frac{R_0}{R_0 + R_L} \right)^2 \sigma_{TX} \sigma_{RX}. \quad (1)$$

The ready availability of high power lasers usually means that the insertion loss of a simple, short haul link is determined by the saturation power of the photodiode receiver. Typically, linear operation of commercially available high speed PIN photodetectors is only guaranteed for incident optical powers of a few milliwatts, leading to values for the RF insertion loss of the order of 55 dB. To overcome this large loss a substantial amount of wide bandwidth preamplification is usually required in a practical link or receiver system—hence the importance

Manuscript received January 16, 1995; revised March 28, 1995.

The authors are with the Defence Science and Technology Organization, Electronic Warfare Division, Salisbury, South Australia 5108.

IEEE Log Number 9413699.

TABLE I  
TYPICAL LINK PARAMETERS

Optical link parameters		
$P_0$	3 mW	
$r$	0.6 mA/mW	
$V_\pi$	12.5 V	
$R_{in}$	$30\Omega$	
$R_0 R_L$	$50\Omega$	
$\alpha_{m1}, \alpha_{opt}$	3.5 dB, 1 dB	
$\alpha_{TX}, \alpha_{RX}$	0.9	
$\rho_G$	-57 dB	Optical link gain
$P_{1dB}$	+24 dB	1 dB Compression (input)
$F_L$	58 dB	noise figure
Preamplifier parameters		
$G$	43 dB	
$P_{1dB}$	+18 dBm (output)	
$F_p$	3 dB	
Cascade link performance		
$G_T$	-14 dB	
$TP_{1dB}$	-23 dBm (input)	
$F_T$	15 dB	

of MMIC technology to the successful implementation of wideband photonic systems.

Table I shows some typical component parameters for the preamplifier and optical link. The RF characteristics of the cascaded components are calculated using standard formulae, discussed in Section II. The total noise figure ( $F_T$ ) of  $\sim 13$  dB implies a system noise floor of about -80 dBm for a 100 MHz detection bandwidth, and therefore a compressive dynamic range of 55 dB. This simple model has been found to yield reasonably accurate estimates for the link performance, typically underestimating the insertion loss by 2-3 dB at the higher microwave frequencies.

### B. Incorporating a Photonic Mixer

If two integrated optical modulators (each with the transfer function (A.1)) are cascaded and biased at quadrature ( $\phi_0 = \pi/2$ ), with each subject to a signal of the general form

$$V_{1,2}(t) = V_{1,2} \sin(\omega_{1,2}t) \quad (2)$$

then the overall transfer function is

$$P_m = \frac{P_0}{4} [1 - \sin(X_1 \sin \omega_1 t) - \sin(X_2 \sin \omega_2 t) + \sin(X_1 \sin \omega_1 t) \sin(X_2 \sin \omega_2 t)] \quad (3)$$

where

$$X_{1,2} \equiv \frac{\pi V_{1,2}}{V_\pi} = \frac{\pi \sqrt{\sigma_{1,2} P_{1,2} R_{1,2}}}{V_\pi} \quad (4)$$

and the electrical matching of the modulator electrodes is taken into account [see, for example, (A.6)]. Contributions from optical losses of the system have been neglected and the nomenclature has been chosen to be consistent with [1].

The Bessel function identity [2]

$$\sin(z \sin \theta) = 2 \sum_{k=0}^{\infty} J_{2k+1}(z) \sin([2k+1]\theta) \quad (5)$$

can be used to express (3) as a harmonic expansion, given by

$$\begin{aligned} P_m = & \frac{P_0}{4} [1 - 2(J_1(X_1) \sin \omega_1 t + J_1(X_2) \sin \omega_2 t)] \\ & + \frac{J_1(X_1) J_1(X_2)}{2} [\cos\{(\omega_1 - \omega_2)t\} \\ & - \cos\{(\omega_1 + \omega_2)t\}] \\ & + \text{terms at frequencies } 3\omega_{1,2} \text{ and } (3\omega_{1,2} \pm \omega_{2,1}) \\ & + \text{higher order terms.} \end{aligned} \quad (6)$$

Thus, incorporating the second integrated optical modulator leads to linear mixing terms at the intermediate frequency (IF)  $\omega_{IF} = \omega_1 - \omega_2$  and the image term at  $\omega_1 + \omega_2$ . Another important feature of (6) is that, unlike the case of using the psuedo-square law response of a microwave diode, there is no contribution to the final output signal corresponding to third-order intermodulation distortion i.e. there are no spurious mixing products at the frequencies  $2\omega_{1,2} \pm \omega_{2,1}$ . This arises due to the fact the response of the cascade modulators is essentially a true multiplication and the transfer function of each individual modulator contains no even harmonics—the mixing is not a result of any nonlinearity in the photodetector response. The absence of the third-order products suggests the possibility of implementing extremely wide bandwidth mixers that have an enhanced dynamic range.

It is worthwhile examining the characteristics of a wide bandwidth, externally modulated fiber optic link which incorporates a second modulator in order to mix a known LO frequency with the incoming RF signal to produce an IF suitable for analysis.

The useful IF signal incident on the photodiode is, from (6)

$$P_{PD} = \frac{J_1(X_{RF}) J_1(X_{LO})}{2} \alpha_{RF} \alpha_{LO} \alpha_{opt} P_0 \cos \omega_{IF} t \quad (7)$$

where the optical loss contributions have been included and the signal  $V_{1(2)}$  has been explicitly identified as the RF (LO) signal. Following the procedures outlined in the Appendix, a small signal approximation for  $J_1(X_{RF})$  is used. This allows terms that correspond to the simple RF link insertion loss  $\rho_G$ , given by (1), to be identified. The efficiency of the total system in downconverting the original RF to the final IF signal can then be expressed as

$$\rho_{IF} = \rho_G \left( \frac{\alpha_{LO}}{2} \right)^2 J_1^2(X_{LO}). \quad (8)$$

Since the LO signal is usually a substantial fraction of  $V_\pi$ , the nonlinear nature of  $J_1(X_{LO})$  should be taken into consideration. Assuming an LO power of +20 dBm and 3 mW of laser power, (8) gives a total input RF to output IF conversion loss of 84 dB. The majority of this loss is associated with the usual transduction loss of a wide bandwidth photonic link, as described by the first two terms (8). The extra electrical penalty of the mixing process is given by the final term of this equation. This suggests that a microwave system model for such a mixer would consist of a normal link parameter calculation which also accounts for the extra optical losses associated with the LO modulator, followed by a virtual mixer with a conversion gain given by the final term of (8).

It is clear from (8) that it is desirable to maximize the LO power in order to minimize the conversion loss. The maximum possible value of  $J_1(X_{\text{LO}})$  is  $\sim 0.58$ , giving  $\rho_{\text{IF}} = -75$  dB for the above example. The maximum value of the Bessel function corresponds to an argument of  $X_{\text{LO}} \sim 1.8$ , which for a  $V_{\pi}$  of 12.5 V establishes a maximum required LO power of the order of +33 dBm. This amount of LO power is very large compared to that required by a wide bandwidth MMIC mixer (typically of the order of 10–13 dBm).

Any further improvement in the conversion loss the link as it stands could only be obtained by improving the optical section, in particular by increasing the optical power. In the above example the average optical power incident on the photodiode will only be 120  $\mu\text{W}$ , which is well below saturation (the example link model assumes there is 8 dB of optical insertion loss, plus there will be a further 6 dB due to having to bias each modulator at quadrature). Increasing the laser power to, say, 40 mW (which can be obtained from sources such as diode-pumped Nd:YAG lasers), will decrease the RF to IF conversion loss to 52 dB. The larger source will result in an average of about 1.6 mW of laser power at the detector, which will be close to the linear limit of most microwave PIN photodiodes.

An important difference between this case and the case of a simple link application is that only the IF signal need be detected, not the original RF signal. Thus the photodiode bandwidth need only be that of the IF bandwidth. This in turn implies that much larger area photodiodes can be used, resulting in

- 1) a larger optical power handling capability and improved optical coupling due to the larger surface area,
- 2) a lower RF to IF conversion loss due to improved optical coupling and increased power capability,
- 3) a cost reduction in the photodiode itself,
- 4) the possibility of improved RF matching techniques due to the smaller detection bandwidth, and
- 5) better RF sensitivity due to the smaller detection bandwidth and lower conversion loss.

### C. Receiver System Analysis—RF Aspects

Having determined the basic expression for the insertion loss associated with the RF to IF down-conversion, it is possible to calculate the effect of the various noise contributions on the sensitivity of the link. The total noise contribution determines the minimum detectable RF signal power. A calculation of the spurious signal content arising from the dominant nonlinearities then gives the maximum RF signal strength corresponding to an unambiguous IF signal that can then be processed by the system. The difference between these two limits gives the link dynamic range. The calculation of these quantities is the subject of this section.

The equivalent input noise power density (EIN) can be estimated from the shot noise of the laser field and the thermal noise of the detector using the formula (see, for example, [3])

$$\text{EIN (dBm/Hz)} = 10 \log \left[ \frac{1}{\rho_{\text{IF}}} \left( kT + \frac{erR_L \bar{P}_{\text{PD}}}{2} \right) \right] + 30 + 4.7 \quad (9)$$

where  $\bar{P}_{\text{PD}}$  is the average laser power incident on the photodiode in Watts.

The first additive constant accounts for conversion from dBW to dBm. There is also an approximation of an extra 4.7 dB noise contribution, which is associated with the folding of uncorrelated noise in the frequency region ( $\omega_{\text{LO}} \pm B_{\text{IF}}$ ) into the IF bandwidth and noise passed straight through at the IF bandwidth due to the broadband response of the link. The contribution from laser random intensity noise (RIN) has been ignored as this is generally well below the thermal and shot noise contributions for systems employing high quality, high power sources such as diode-pumped solid state lasers (which need to be used due to the conversion loss considerations discussed previously).

From a systems viewpoint, the link noise figure  $F_L$  is often used. The link noise figure is the ratio of the link EIN to the thermal noise, i.e.

$$F_L(\text{dB}) = \text{EIN (dBm/Hz)} + 174(\text{dBm/Hz}). \quad (10)$$

The system noise floor is then given by

$$S(\text{dBm}) = -174(\text{dBm/Hz}) + F_L(\text{dB}) + 10 \log B_{\text{IF}}. \quad (11)$$

Assuming  $B_{\text{IF}} = 100$  MHz and  $F_L = 60$  dB, (11) implies a noise floor of only  $-34$  dBm for the example optimized system. This sensitivity is inadequate for many defence applications and as such wide bandwidth preamplification will be necessary in order to realize an acceptable sensitivity. The use of such an amplifier will however have an impact on the overall system dynamic range, which must be taken into consideration.

Equation (11) determines the limit for the *smallest* input signals that can be detected at the IF output of the link. The amplitude of the *largest* signals that can be processed will be determined by the dominant nonlinearities in the link. In a normal diode mixer the major contributing factor would be the spurious third-order artifacts formed by mixing the strong LO with the RF signal. Since there are no third-order intermodulation products from the mixing process, the maximum signal that can be processed unambiguously will be limited by either the generation of third-order products due to the simultaneous arrival of two signals on the RF modulator, or a single large amplitude signal forcing the RF modulator into compression. These limiting cases define the *spur-free dynamic range* (SFDR) and the *compressive dynamic range* (CDR) respectively.

Thus the dynamic range of the optical section of the link will be limited at high RF powers by the usual nonlinearity of the RF modulator. The maximum average input power can be characterized by either the *1-dB compression point* ( $P_{1\text{dB}}$ ) or *the third order intercept* (TOI), which are given by [4]

$$P_{1\text{dB}} = \frac{\rho_{\text{IF}}}{2R_{\text{in}}} \left( \frac{0.933V_{\pi}}{\pi} \right)^2 \text{ Watts} \quad (12)$$

$$\text{TOI} = P_{1\text{dB}} + 9.6 \text{ dB.} \quad (13)$$

The inclusion of  $\rho_{\text{IF}}$  in (12) refers  $P_{1\text{dB}}$  to the output of the link. Equation (13) is a general approximation often used to

estimate the TOI from  $P_{1\text{dB}}$  for any microwave component. The SFDR and CDR can be related to  $P_{1\text{dB}}$  and the TOI by

$$\text{SFDR} = \frac{2}{3}(\text{TOI} - S) \quad (14)$$

$$\text{CDR} = P_{1\text{dB}} - S \quad (15)$$

where  $S$  is the system noise floor, given by (11).

The photonic mixer can now be treated as a system “black box”, with its performance defined by the parameters  $\rho_{\text{IF}}$ ,  $F_L$ , and  $\text{TOI}_L$ . Knowing the equivalent parameters for all other link components (amplifiers etc.), the standard component cascade formulae can be used to estimate the overall link performance. These are given in (16) and (17) for the case of a three component system

$$F_T = F_1 + \frac{F_2 - 1}{G_1} + \frac{F_3 - 1}{G_1 G_2} \quad (16)$$

$$\text{TOI}_T = \left( \frac{1}{G_3 G_2 \text{TOI}_1} + \frac{1}{G_3 \text{TOI}_2} + \frac{1}{\text{TOI}_3} \right)^{-1} \quad (17)$$

where the  $F_i$  are the individual component noise figures, the  $G_i$  are the individual component *available* gains and all of the TOI's are referred to the *output* of each link component. All quantities are in linear units. The cascaded link parameters given in Table I were calculated using these formula. Care must be taken when using (16) and (17), since it is device *available* gain that is used, whereas it is *insertion gain* that is normally measured [5].

It is important to note that the preamplifier needs to have a high 1-dB compression point ( $>\sim 20$  dBm) if it is not to be responsible for limiting the dynamic range, rather than the nonlinear characteristics of the RF modulator. Thus, one of the potential advantages of the photonic mixer—that of increased dynamic range due to reduced third-order intermodulation distortion—may not be realized in some circumstances due to other system considerations. Nonetheless, the absence of spurious third-order signals that would otherwise increase the post-processing load is still a significant advantage of the photonic mixer architecture.

If the intent is to construct an EW receiver system which incorporates a photonic mixer, it is necessary to convert the IF information into a video signal suitable for electronic processing. Therefore a video detection stage must be incorporated after the IF stage. The inclusion of the video detection process must be correctly modelled as it has a significant effect on the sensitivity criteria and operational bandwidth of the receiver system.

#### D. Receiver System Analysis—Video Aspects

The necessity for electronic processing following video detection means that a different sensitivity criteria to that of the system noise floor is used. The simplest criterion is known as the *tangential signal sensitivity* (TSS).

The TSS is only defined for pulsed RF input signals, and can be determined by displaying the resulting output video pulses on an oscilloscope. The TSS is the input power level which results in an output where the top of the noise at the baseline is at the same level as the bottom of the noise on the video pulse. This can be a very subjective measurement and hence it

is useful to have an analytical expression. From [6], which is based on defining TSS as the input power level corresponding to an output S/N ratio of 8 dB, an appropriate expression is

$$\text{TSS (dB)} = -114 + 10 \log F_T + 10 \log (2.5 \sqrt{2B_R B_V}) \quad (18)$$

where the leading constant is simply the thermal noise referred to a 1 MHz bandwidth,  $F_T$  is the total noise figure prior to the detector,  $B_R$  is the RF bandwidth (MHz) prior to the detector (in this case the IF bandwidth) and  $B_V$  is the video bandwidth (MHz) after the detector,

This expression is applicable to a narrow band superheterodyne architecture with  $B_V \ll B_R$ . This leads to the concept of an effective detection bandwidth  $B_e$  given by the last term in (18).

It is the effective bandwidth that should be used when determining the noise floor  $S$  at any point further forward in the system, rather than  $B_{\text{IF}}$ . Similarly, the SFDR and CDR should correctly be calculated using the TSS as the minimum detectable signal, rather than the usual system noise floor  $S$  as determined from the cascaded EIN of the RF section of the system.

### III. SYSTEM IMPLEMENTATION

#### A. Mixer Characterization

In order to validate the modelling of the previous section, a 20-GHz bandwidth superheterodyne receiver architecture incorporating a photonic mixer was constructed. The experimental arrangement is shown in Fig. 2.

The initial stage of the project was to characterize the photonic mixer. The RF sources were an 18.6-GHz dielectric resonator oscillator (DRO) and a 40-GHz Wiltron 6769A frequency synthesizer. The DRO was amplified to +22 dBm using a 19-GHz medium power amplifier, and the RF signal amplified to +10 dBm. Both sources were filtered to minimize unwanted harmonic content. The resulting second harmonic was  $< -80$  dBc.

The optical source was a  $1.32 \mu\text{m}$ , 43 mW diode-pumped Nd:YAG laser which was fiber coupled to two cascaded, 20 GHz bandwidth United Technologies integrated optical modulators. Each modulator was preceded by a polarization controller and followed by a power monitoring port. The detector was a 25-GHz New Focus photodiode. The signal directly from the detector was displayed on an HP8564E 40-GHz spectrum analyzer.

The total optical insertion loss for the link was measured to be 10 dB. Assuming other standard values for link parameters the calculated RF insertion loss of the cascaded modulators biased at quadrature was 51 dB, with an extra RF to IF conversion loss of 12 dB. The measured values were 54 and 12 dB respectively, as shown in Fig. 3. The expected linear mixing products at  $\omega_{\text{IF}} = 10$  GHz and the upper sideband at 27.2 GHz are apparent. The IF of 10 GHz was chosen simply to illustrate the wide band nature of the mixer.

Fig. 4 shows the results obtained for the measurement of the third order intermodulation product, which should occur at 1.4 GHz. The lower trace is with the modulators correctly biased.

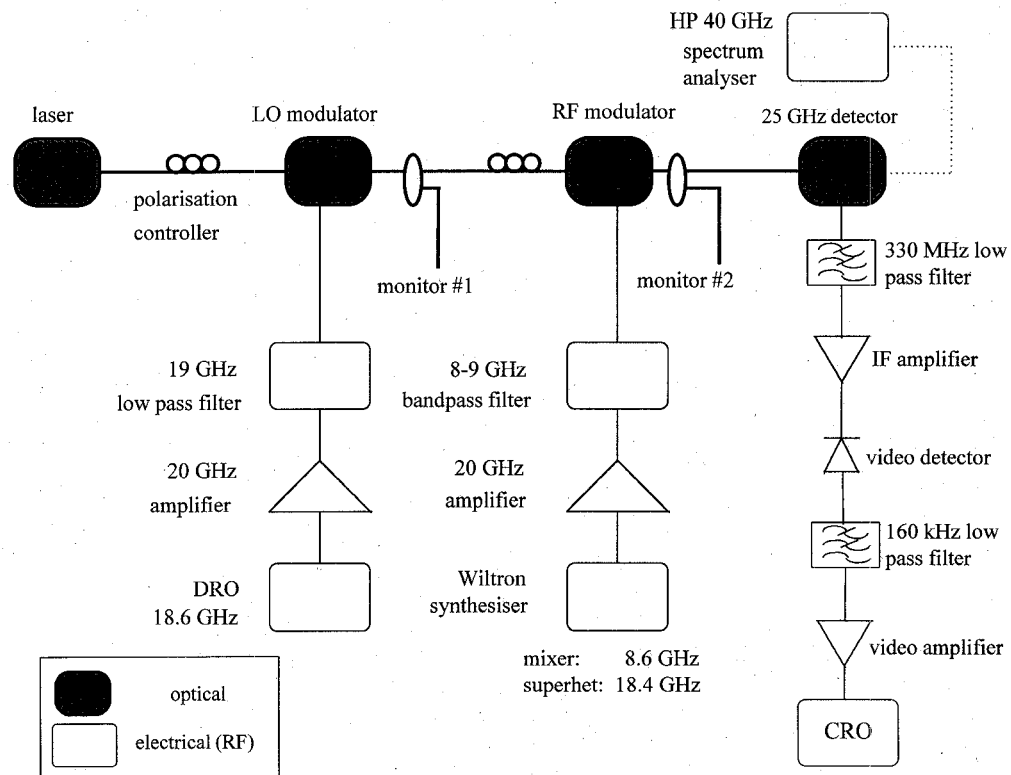


Fig. 2. Experimental arrangement for mixer and superheterodyne receiver characterization.

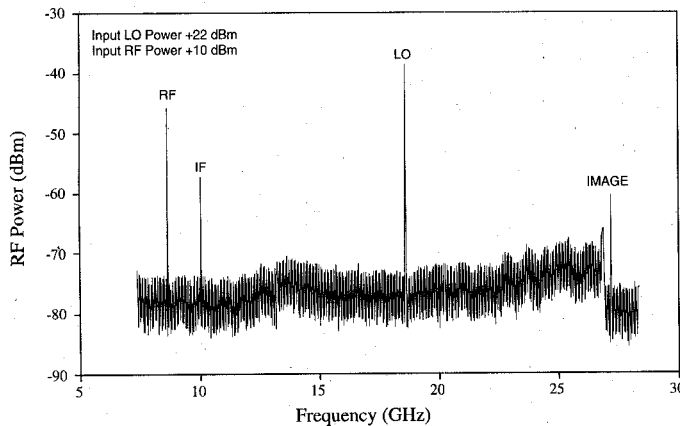


Fig. 3. Output from photonic mixer showing RF, LO, IF and image frequencies.

The upper trace shows the position of the intermodulation product, which was introduced by deliberately de-biasing one modulator. It is clear that the unwanted third-order products can be eliminated to better than 70 dB below the valid IF signal. This level of spurious signal rejection is considerably better than that achieved by standard electronic mixers.

#### B. Receiver Characterization

The second stage of the project was to incorporate the mixer into a simple superheterodyne architecture.

The RF source was set to produce 50  $\mu$ s pulses at a center frequency of 18.4 GHz, giving a 200-MHz IF output from the optical link. The photodetector was followed by a 330-MHz

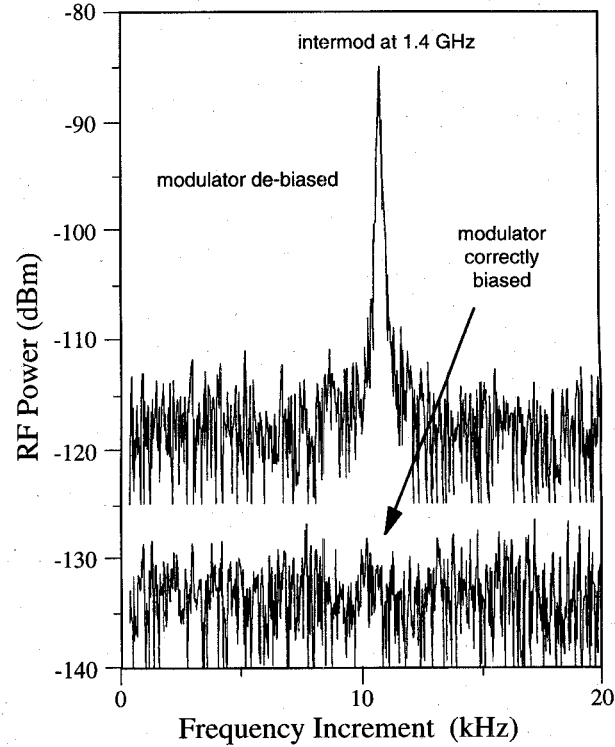


Fig. 4. Measurement of intermodulation product. The upper trace has been offset by 15 dB, and shows the presence of the intermodulation term when the modulator is deliberately debiased.

low pass filter and a further 43 dB of IF amplification. The final IF signal was detected on a Wiltron75N50B microwave diode, amplified by a 0.16-MHz bandwidth amplifier and then dis-

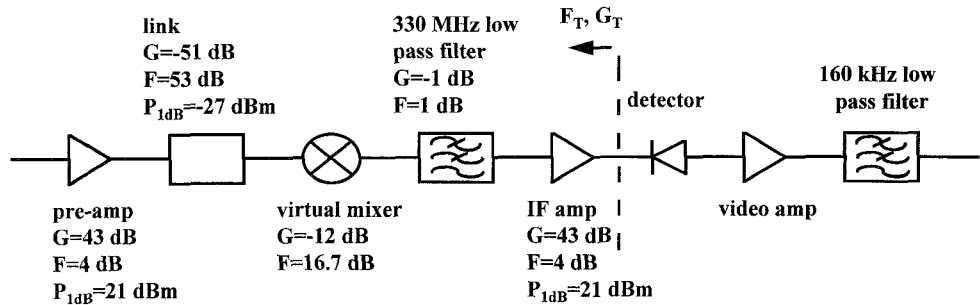


Fig. 5. Equivalent RF system model for a link incorporating a photonic mixer.

played on a Tektronix 2465B oscilloscope. This arrangement essentially results in a superheterodyne receiver with a 660-MHz signal resolution bandwidth, due to the fact that signals falling 330 MHz either side of the LO frequency will be folded into the same IF band. The effective noise bandwidth, from (18), is 26 MHz.

The equivalent RF system model is shown in Fig. 5.

The TSS and  $P_{1\text{dB}}$  were measured to be  $-66$  and  $-22$  dBm. These figures imply a CDR of  $44$  dB and a SFDR of  $36$  dB. These results are to be compared with the calculated values of  $\text{TSS} = -73$  dBm,  $P_{1\text{dB}} = -24$  dBm, CDR =  $49$  dB, and SFDR =  $39$  dB, obtained using the formulae of Section II.

Most of the discrepancy between the simple model predictions and the actual measurements is due to the extra  $3$  dB insertion loss of the link. This is believed to arise due to the frequency dependence of  $V_\pi$ , which results in increased insertion loss at high microwave frequencies. Inserting the measured values into the system equations of Section II yields a  $\text{TSS} = -70$  dBm. In this case the calculated system noise figure of  $30$  dB also corresponds reasonably well with the measured noise figure of  $34$  dB.

#### IV. SYSTEM IMPROVEMENTS

It is clear that the receiver as demonstrated is not competitive with normal superheterodyne receiver technology. The dynamic range in particular is quite poor. There are a number of system improvements which can be made, including: decreasing the modulator  $V_\pi$ , increasing the LO power, increasing the optical power, improving the linearity of both the preamplifier and the transfer characteristic of the RF modulator, accounting for antenna gain, reducing the IF bandwidth, and using narrow band photodiodes to detect the IF component.

In particular, exploiting low speed photodiodes may provide substantial system improvements. Since only the IF frequency needs to be detected, a larger area PIN or avalanche photodiode can be used. The larger tolerable RC time constant means that the photodiode could be matched into a high impedance load. The resulting signal could then be buffered to a very small output impedance, thereby resulting in a net power gain into a standard  $50\ \Omega$  load. A simple circuit of this type and costing only a few dollars was shown to reduce the total RF to IF conversion loss of the photonic mixer by  $15$  dB.

Further substantial improvements in performance can be achieved by designing low  $V_\pi$  modulators. Significantly im-

proving the  $V_\pi$  will result in reduced link insertion loss, however considerations such as modulator linearization become an issue, since the dynamic range will be limited by the nonlinearity of the electrooptic modulator.

The fundamental limitation in using photonic mixers to produce wide bandwidth superheterodyne receiver architectures lies in the large insertion loss of the link. The limited power handling capability of current commercially available photodiodes and the inefficiency of the RF to optical transduction process lead to the requirement for high gain, wide bandwidth preamplification, which therefore limits the dynamic range of the system.

Thus, while normal electronic mixers may suffer from the presence of intermodulation levels well in excess of those exhibited by the photonic mixer, other system considerations mean that the dynamic range of the photonic superheterodyne system is less than that of a conventional system.

The above observations hold when considering photonic superheterodyne systems that have to operate over very large frequency ranges and wide IF bandwidths. Systems that only need to operate over much smaller frequency ranges and narrower bandwidths may exhibit significant improvement over conventional architectures.

If the system improvements can be realized, the photonic receiver has the advantages of:

- 1) no spurious third-order intermodulation products from the mixing process,
- 2) no harmonic or intermodulation products associated with even multiples of either the LO or the RF,
- 3) well-defined amplitude relationships between the required signal and existing spurious signals,
- 4) infinite isolation between the RF and LO ports with no possibility of re-radiation of the strong LO signal.

In an electronic warfare environment, these advantages will often have a significant impact on the operational utility of the technology.

#### V. CONCLUSION

A 20-GHz photonic RF mixer has been constructed and demonstrated. The third-order intermodulation products were shown to be more than  $70$  dB below the IF signal. The advantages of such a mixer include reduced post-processing load due to minimal spurious signal generation, and infinite isolation between the RF and LO ports. An increase in the dynamic range of a receiver incorporating such a mixer may be possible,

especially over smaller bandwidths of operation. In the case of large bandwidth receivers other system considerations may limit the dynamic range.

The mixer was then incorporated into a simple 20 GHz scanning superheterodyne receiver architecture with a resolution bandwidth of 660 MHz. The receiver was demonstrated to have a tangential sensitivity of -66 dBm and a compressive dynamic range of 44 dB. A number of system improvements were discussed.

## APPENDIX

### BASIC RF LINK INSERTION LOSS CALCULATION

The optical intensity versus voltage relationship for the interferometric modulator is [1], [3]

$$P_m = \frac{P_0 \alpha_m}{2} \left( 1 + \cos \left[ \phi_0 + \frac{\pi V(t)}{V_\pi} \right] \right) \quad (A1)$$

where  $P_0$  is the incident optical power,  $\alpha_m$  is the modulator loss,  $\phi_0$  is an intrinsic phase bias,  $V_\pi$  is the half-wave voltage of the modulator, and  $V(t)$  the input signal. Choosing the bias such that  $\phi_0 = \pi/2$ , (A1) can be written

$$P_m = \frac{P_0 \alpha_m}{2} \left( 1 - \sin \left[ \frac{\pi V_{in} \sin \omega t}{V_\pi} \right] \right). \quad (A2)$$

Using the identity (3), and the small-signal approximation  $J_1(X) \approx X/2$  (since  $V_{in} \ll V_\pi$ ), (A2) becomes

$$P_m = \frac{P_0 \alpha_m}{2} \left( 1 - \left[ \frac{\pi V_{in}}{V_\pi} \right] \right). \quad (A3)$$

Ignoring the dc term, the useful power incident on the photodiode is

$$P_{pd} = \frac{\pi P_0 \alpha_m \alpha_{opt} V_{in}}{2 V_\pi} \quad (A4)$$

where  $\alpha_{opt}$  is the optical loss due to splices, connectors etc.

From Fig. 1, the output power (electrical) delivered to the load is therefore

$$P_{out} = \left( \frac{\pi r P_0 \alpha_m \alpha_{opt}}{2 V_\pi} \frac{R_0}{R_0 + R_L} V_{in} \right)^2 R_L \quad (A5)$$

where  $r$  is the responsivity of the photodiode (A/W) and the photodiode is assumed to operate as a linear device.

The input voltage  $V_{in}$  is related to RF input power by

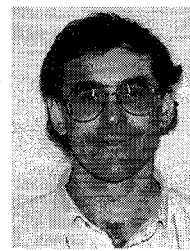
$$V_{in}^2 = (1 - |\Gamma|^2) P_{in} R_{in} = \sigma^{tx} P_{in} R_{in} \quad (A6)$$

where  $|\Gamma|$  is the input voltage reflection coefficient magnitude and  $\sigma_{TX}$  is the transmitter power matching coefficient. Thus, the link gain can be written as

$$\rho_G = R_{in} R_L \left( \frac{\pi r P_0 \alpha_m \alpha_{opt}}{2 V_\pi} \right)^2 \left( \frac{R_0}{R_0 + R_L} \right)^2 \sigma_{TX} \sigma_{RX}. \quad (A7)$$

## REFERENCES

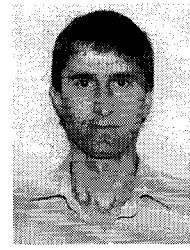
- [1] G. K. Gopalakrishnan, W. K. Burns, and C. H. Bulmer, "A LiNbO<sub>3</sub> microwave-optoelectronic mixer with linear performance," in *IEEE MTT-S Dig.*, 1993, pp. 1055-1058.
- [2] See, for example, M. Abramowitz and I. A. Stegun, Eds., *Handbook of Mathematical Functions*. New York: Dover, 1970.
- [3] R. Simons, *Optical Control of Microwave Devices*. Boston: Artech House, 1990.
- [4] D. D. Hall, M. J. Wale, C. Edge, and N. J. Parsons, "Advances in microwave optoelectronics," *GEC J. Res.*, vol. 10, no. 2, pp. 80-84, 1993.
- [5] HP Application Note 57-1, "Fundamentals of RF and microwave noise figure measurements," Hewlett Packard 1983, pp. 10-11.
- [6] J. Tsui, "Tangential sensitivity of EW receivers," *Microwave J.*, Oct. 1981, pp. 99-102.



**Anthony C. Lindsay** (M'90) received the B.Sc. degree (Hons.) in 1984 and the Ph.D. degree from the James Cook University of North Queensland, Australia, in 1989.

In 1988 he joined the Defence Science and Technology Organization, where his main work has been in advanced optical signal processing techniques for microwave, millimeter-wave and communications EW. He is currently a Senior Research Scientist in the Electronic Warfare Division, with research interests in ultrafast optoelectronics and wide bandwidth, analogue microwave/mm-wave photonics.

Dr Lindsay is a member of the Optical Society of America.



**Geoff A. Knight** (M'95) received the B.Sc. (computer science) degree and the B.E. (electrical engineering) degree from Sydney University, Australia, in 1983 and 1985, respectively.

From 1985-1986 he worked for the Overseas Telecommunications Commission Australia in the field of satellite communications. Since 1986 he has been with the Electronic Warfare Division of the Defence Science and Technology Organization, Salisbury, South Australia. During this period he has been involved in microwave and millimeter-wave component and system engineering. His research interests include millimeter-wave wideband MMIC and photonic technology.



**Steven T. Winnall** (S'94) received the B.E. degree with honors in electronic engineering from the University of Adelaide in 1994.

He is currently employed in the Advanced Concepts Group of the Electronic Warfare Division, Defence Science and Technology Organization Australia. His current research interests include microwave and photonic component and system design.